Inhibitors of spinal cord regeneration

Ehlert, E.M.E.

2011

document version
Publisher's PDF, also known as Version of record

CHAPTER 6

Genetic mutation of the class-3 semaphorin receptor component Npn-2 does not enhance rubrospinal tract regeneration

Erich M Ehlert, Ruben Eggers and Joost Verhaagen

manuscript in preparation

Abstract

After spinal cord injury, axon outgrowth inhibitors present in myelin and in the neural scar are considered to contribute to the failure of injured axons to re-establish functional connections. Class-3 semaphorins are expressed by the meningeal cells that infiltrate the glial scar after injury and signal by binding to neuropilin-1 (Npn-1) or neuropilin-2 (Npn-2). Since neurons of the red nucleus express only Npn-2, rubrospinal axons of Npn-2 knock out (KO) animals should be insensitive to all class 3 semaphorins. To examine the effect of genetic deletion of Npn-2 on the inability of rubrospinal tract (RST) axons to regenerate, we have analysed RST regeneration in Npn-2 KO and wild type littermates. In this study we report that Npn-2 deficient mice do not exhibit improved RST axon outgrowth and do not show enhanced recovery of motor function.

Introduction

Following spinal cord injury (SCI), most injured neurons fail to regenerate and do not re-establish functional synaptic connections. The virtual lack of a growth response in vivo is, at least in part, caused by the presence of growth inhibitory molecules in the spinal cord and at the lesion site. These growth inhibitory molecules include myelin-associated inhibitors and scar-associated molecules such as chondroitin sulphate proteoglycans and chemorepulsive axon guidance molecules (reviewed by Giger 2010, Niclou et al. 2006, Fawcett 2006, Bolsover 2008).

Semaphorins are chemorepulsive guidance molecules originally identified as repulsive cues that act during development of the nervous system (Kolodkin *et al.,* 1993, Luo *et al.,* 1993). The semaphorin family is comprised of a large number of membrane-bound and secreted proteins, subdivided in eight classes of invertebrate semaphorins (class 1 and 2), vertebrate semaphorins (class 3-7) and viral semaphorins (class V) (reviewed by Pasterkamp and Giger). The secreted class 3 semaphorins, with the exception of Sema3E, bind to the neuropilin (Npn) receptor and signal through a plexin class-A (PlxA) signal transducing subunit (Yaron *et al.,* 2005). Two Npn receptors have been identified (Chen *et al.,* 1997, He and Tessier-Lavigne, 1997, Kolodkin *et al.,* 1997). Sema3A exclusively binds to Npn-1 while Sema3C binds predominantly and 3F exclusively to Npn-2 (He and Tessier-Lavigne, 1997, Kitsukawa *et al.,* 1997, Kolodkin *et al.,* 1997, Chen *et al.,* 1998, Giger *et al.,* 1998b, Renzi *et al.,* 1999).

After SCI, class 3 semaphorins are (re-)expressed at the site of injury. In the lesioned spinal cord they can have at least two possible functions. First, following SCI, the meningeal cells that invade the core of the lesion site, express the secreted class 3 semaphorins Sema3A, 3B, 3C, 3E and 3F (Pasterkamp *et al.,* 1999a, Pasterkamp *et al.,* 2001, De Winter *et al.,* 2002b). Most injured spinal cord neurons continue to express class 3 semaphorin receptor components (De Winter *et al.,*

2002b, Spinelli *et al.,* 2007). The presence of semaphorins is likely to contribute to the growth inhibitory properties of the neural scar. Moreover, oligodendrocytes express the membrane-associated Sema4D and 5A (Cohen *et al.,* 2003, Moreau-Fauvarque *et al.,* 2003). The semaphorins produced by oligodendrocytes could act in concert with the classical myelin-associated inhibitors to inhibit axon regeneration. Second, semaphorins may affect the formation of the neural scar by influencing scar-associated cell migration, proliferation and neovascularisation (Chedotal, 2007, Joyal *et al.,* 2011).

The presence of class 3 semaphorins in the neural scar and their potential contribution to the inhibition of axonal regeneration, suggest that interfering with semaphorin signalling could be beneficial to spinal cord regeneration. In chapter 5 we have investigated the role of Sema3A during corticospinal tract (CST) regeneration by selective mutation of Npn-1 in neurons. This study showed that knocking out Npn-1 did not improve CST fiber regeneration and did not improve motor function. In chapter 5 we discuss several factors that may underlie the lack of improved recovery in these conditional Npn-1 animals. One of the possible explanations is that corticospinal neurons express both Npn-1 and Npn-2 (De Winter *et al.,* 2002b). Knocking out Npn-1 alone does therefore not abrogate all scar derived repulsive Sema3 signals. Since neurons of the red nucleus express only Npn-2 (De Winter *et al.,* 2002b), rubrospinal axons of Npn-2 KO animals should be insensitive to all class 3 semaphorins. To study the effect of genetic deletion of Npn-2 on the failure of injured RST axons to regenerate, we have analysed rubrospinal tract (RST) regeneration and functional motor behaviour after unilateral lesion of the RST in Npn-2 KO mice. We show that after an RST lesion, disruption of Npn-2 signalling does not improve outgrowth of RST axons and does not lead to enhanced recovery of motor function.

Methods

Experimental animals

The Npn-2 knockout mice were provided by Dr Roman Giger (University of Michigan, MI, USA). The animals were maintained as Npn-$2^{+/-}$ heterozygous animals in a C56BL/6 background. Npn-$2^{-/-}$ KO animals were obtained by heterozygous Npn-$2^{+/-}$ intercrossings. Wild type (WT) littermates were used as control animals. Animals were housed in groups under standard conditions with food and water ad libitum and a 12h:12h light/dark cycle. Experimental procedures and behavioural tests were performed in accordance with the committee for laboratory animal welfare and experimentation of the Royal Netherlands Academy of Sciences.

Animal surgery

RST transection: Animals were deeply anesthetized by an intraperitoneal injection of Hypnorm (0.1 mg/kg Fentanyl citrate/ 3.3 mg/kg Fluanisone HCl, Janssen Pharmaceuticals) and Dormicum (8.3 mg/kg Midazolam, Roche). During surgery, body temperature was maintained at 37°C using a heating pad. The spinal cord was exposed by partial laminectomy of the C4 vertebra. The dura mater was opened using Vannas scissors followed by a unilateral lesion of the left dorsal horn using a micro knife transecting the RST. Muscle layers were sutured and the skin was closed with Michell clips (Fine science tools). Postoperative analgesia was administered by one single subcutaneous injection of Metacam (0.4 mg/kg, Boehringer Ingelheim). In animals of the sham procedure group a laminectomy was performed leaving the dura matter and spinal cord intact.

RST tracing: RST fibers were anterogradely traced four weeks after surgery. To this end animals were anesthetized as described before and 0.8 µl of biotinylated dextran amine (BDA) solution (10% in PBS, MW 10.000, Invitrogen) was infused into the red nucleus (coordinates; AP: -3.5 mm, L: -0.5 mm from lambda, DV: -3.5 mm from dura) at a flow of 0.2 µl/min.

Experimental groups: All animals were 13 to 17 weeks of age on the day of surgery. A total of 12 KO and 14 WT mice received a unilateral RST lesion. The sham group consisted of 4 WT mice.

Behavioural testing and evaluation

All animals were tested 3 days before and 3, 7, 10, 14, 17, 21, 24 and 28 days after surgery.

Narrow beam walk: To evaluate recovery of proper hind limb placements after RST lesion, a narrow beam test was performed. Animals were pre-trained for one week to cross an 8 mm wide, 100 cm long and 15 cm elevated beam. The narrow beam was flanked on both sides by a platform from which the animals initiated their run voluntarily. The total number of slips and steps of the left hind limb were counted and averaged from 3 successful runs by two observers blinded to the experimental group.

Rotarod: To assess overall motor coordination, animals were placed on the Rotarod (Ugo Basile Biological Research Apparatus) rotating at a constant speed of 5 rpm. The rotation was accelerated to 40 rpm over a period of 5 minutes. The time the mice could remain on the rotating beam was recorded and normalised for the maximum performance at 3 days before surgery.

Cylinder test: We analysed forelimb motor behaviour by making use of the natural exploratory behaviour of the animals using the cylinder test (Liu *et al.,* 1999). After an animal was placed in a 6 cm diameter glass cylinder, the animals spontaneously started exploring the vertical surface by rearing to a standing position using one or both of its forepaws for support. For the duration of 5 minutes or 20 events we scored the placement of right, left or both forepaws. An event started when the animal reared to a standing position, bearing body

weight with its hind limbs, and supporting the upright position with a weight bearing contact of one or two fore paws with the vertical surface. The event was ended when the animal landed on either one or both fore paws. A single front paw placement was defined as the weight bearing use of the right or left front paw for support in the upright position. The use of both front paws was scored when the animal used both paws consecutive or simultaneously for weight bearing support within one event.

Catwalk gait analysis: Gait analysis was preformed as described before (Hamers *et al.,* 2001). Briefly, mice were pre-trained for one week to cross a 100 cm long glass plate, confined by Plexiglas walls 35mm apart in a darkened room. Paw prints were recorded digitally and analysed using the Catwalk software. All analysed parameters were normalised for the performance at 3 days before surgery.

Tissue preparation

One week after RST tracing, animals were euthanized by injecting an overdose of Nembutal (sodium pentobarbital, Sanofi Sante) followed by transcardial perfusion of ice-cold saline followed by 4% paraformaldehyde (PFA) in 0.1 M phosphate-buffer. The spinal cord and brain were dissected and post fixed overnight at 4°C followed by incubation in phosphate buffered saline (PBS) containing 0.25M EDTA and cryopreservation in PBS containing 25% sucrose. Tissue was embedded in OCT compound (Sakura), snap frozen in 2-methylbutane and stored at -80°C until sectioning. Twenty µm thick transversal cryosections at cervical level C1 were thaw mounted on Superfrost Plus slides (Fisher Scientific). The C2-C6 spinal cord segment was cryosectioned sagitally. All sections were dried and stored at -80°C until use.

Histological analysis and quantification

To determine the total number of BDA traced RST fibers, transversal sections were incubated in Tris-buffered saline (TBS), 0.2% Triton X-100, 5% bovine serum (block buffer) for 1 hour followed by incubation with streptavidin-Alexa488 (1:400, Invitrogen) in blocking buffer for 3 hours at room temperature. The sections were washed three times in TBS containing 0.1% Triton X-100. Tiled images of the dorsal column were captured using an Axioplan 2 microscope (Zeiss) with a 40x objective. The RST was outlined using Imagepro Plus (MediaCybernetics) and a grid was placed over the outlined area. Fibers were counted in approximately 25% of a systematic randomized selection of the outlined area.

To quantify the RST fibers rostral en caudal to the lesion site, we prepared sagittal sections of the cervical C2-C6 region of the spinal cord. The sections were blocked as described above and incubated overnight at 4°C with Rabbit-anti-GFAP (1:1000, DAKO) in block buffer. The following day, sections were

washed three times in TBS containing 0.1% Triton X-100 and incubated with goat anti-Rabbit-Cy3 (1:400, Jackson Immunoresearch) and streptavidin-Alexa488 (1:400, Invitrogen) for 3 hours at room temperature. The sections were washed 3 times in TBS containing 0.1% Triton X-100 and coverslipped. Tiled images were captured from every second section using an Axioplan 2 microscope (Zeiss) with a 20x objective. Using the GFAP IHC signal, the ventral, caudal and rostral borders of the lesion site were identified. Using these three reference points, the center of the lesion was determined. In all images containing BDA positive RST fibers and lines were placed in dorsal-ventral orientation in the core of the lesion and 0.25, 0.50, 0.75 and 1.0 mm rostral and caudal from the lesion center using Imagepro Plus (MediaCybernetics). The number of RST fibers running through the white matter that crossed these lines was counted. The fiber index was calculated by dividing the fiber counts at the set intervals in the C2-C6 lesion area by the total number of fibers at C1 level.

Statistics

All results are expressed as mean ± SEM. For the RST fiber index, narrow beam and cylinder test, statistical significance was tested with a Kruskal-Wallis test followed by a Mann-Whitney U post hoc test. The rotarod and catwalk experimental data were tested with an ANOVA analysis with a Bonferroni post hoc test. A value of $p < 0.05$ was considered significant.

Results

Animal breeding and peroperative mortality of Npn-2 knockout mice

Npn-2 KO mice were obtained using a heterozygous breeding scheme. In our colony of 325 animals that survived into adulthood, 5.8% were of the Npn-$2^{-/-}$ genotype, 48.5% and 35.7% were Npn-$2^{+/-}$ and Npn-$2^{+/+}$ respectively. As reported previously, this clearly indicates a phenotypic effect on the survival rate of neonatal KO mice (Giger *et al.*, 2000). The homozygous KO animals that survived into adulthood had an average decreased body weight of 16 % as compared to their heterozygous littermate as reported previously. To analyse RST regeneration, we performed a unilateral RST lesion at cervical level C4. During this surgical procedure, 5 out of 12 knock out animals (42%) died, where in the wild type group 2 out of 12 (17%) died perioperative.

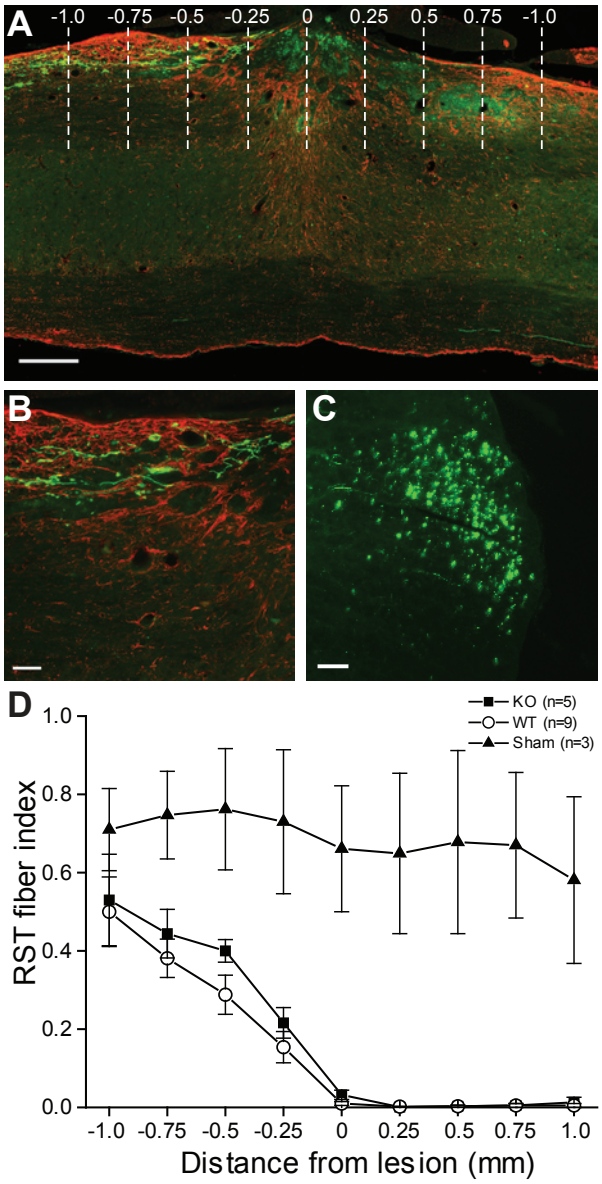

Figure 1. RST fibers regeneration is not enhanced in Npn-2 knockout animals. Immunohistochemical double staining was used to visualize BDA traced RST fibers (green) and GFAP (red) in sagittal sections in the lesioned area (a, b). The total amount of RST fibers at cervical level C1 (c) was used to correct for tracing variability. Quantification of RST fibers at set intervals of the injury site (d) revealed no differences between wild type and knockout animals. Scale bar: 250 µm (a) and 50 µm (b,c).

Histological analysis of RST fibers

To analyse the regenerative response of the rubrospinal fibers, we traced the RST by injection of BDA in the lesioned red nucleus. The animals were sacrificed one week after tracer injection, and tissue was processed for immunohistochemical analysis. Due to tissue handling and cryosectioning procedure error, full histological analysis was possible on 5 KO, 9 WT and 3 sham lesioned animals. The number of RST fibers at 0, 0.25, 0.5, 0.75 and 1 mm rostral and caudal to the lesion site were counted (Fig. 1a,b). To correct for variation of tracing efficiency, the fiber index (Fig. 1d) was calculated by dividing the fiber counts by the total number of traced RST fibers at cervical level C1 (Fig. 1c). The fiber index at 1 mm rostral to the lesion was similar for KO and WT animal. The KO animals show a small trend of increased RST fibers growing towards the lesion. At 0.5 mm rostral to lesion the difference between the regenerating fiber index reaches a maximum of 0.40 ± 0.03 and 0.28 ± 0.05 in KO and WT animals respectively. However, this trend of an increased number of regenerating axons did not reach statistical significance.

Behavioural analysis

The rubrospinal tract plays an important role in voluntary movement of front and hind limbs. A unilateral lesion of the RST at cervical level C4 results in significant motor impairment of the ipsilateral paws. To analyse the loss and regain of motor function in RST lesioned KO and WT mice, we conducted several functional tests.

Narrow beam walk

We examined coordinated hind paw placement of Npn-2 KO and WT animals using the narrow beam walk. After one week of pre-training, all animals crossed the 8 mm wide beam making less than 2% slips or misplacements of the left hind limb. Lesioning the left RST resulted in 82.0 ± 7.6% and 83.4 ± 10.5 incorrect left hind paw placement at 3 days after surgery for KO and WT animals respectively (Fig. 2). Seven days after RST lesion, the incorrect foot placement in the WT animal group decreased to 75.1 ± 7.3% while the KO group increased to 91.3 ± 8.3 % reflecting a significantly difference between the WT and KO group. The WT animals continued to recover to 61.4 ± 8.7% at 14 days after injury and maintained this level of performance throughout the remainder of the experiment. The knockout animals recovered to only 74.0 ± 11.5% at 10 days post injury. From seven days post injury onwards, an average difference of 12% in paw placement error rate of KO animals compared to the WT group persisted throughout the experiment, but did not reach statistical significance.

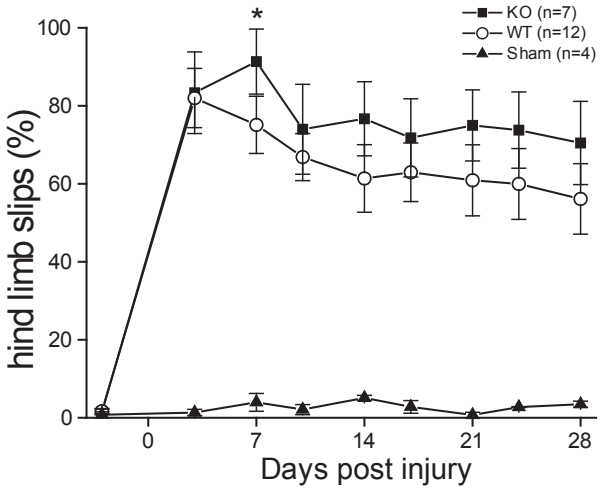

Figure 2 Narrow beam walk analysis shows decreased coordinated hind paw placement in Npn-2 knock out mice. Three days after lesion of the left RST, Npn-2 KO and WT mice made 82.0 ± 7.6% and 83.4 ± 10.5 left hind limb slips respectively. On day 7 after injury, the percentage of slips further increased in KO animals to 91.3 ± 8.3 %, where wild type animals improved hind paw placements to 75.1 ± 7.3%. From this point on, a trend of decreased coordinated hind paw placement in KO animals remained throughout the experiment (p<0.05 significance between KO and WT)*

Rotarod

Coordinated limb movement was analysed using the Rotarod system (Fig. 3). Three days after RST injury, all animals showed a decreased performance as compared to sham-operated animal. Unexpectedly, KO animals showed a significantly larger deficit (43.8 ± 3.9%) than WT animals (64.9 ± 4.2%). Over the following 3 days, WT animals gradually recovered, reaching a plateau at 14 days post injury (88.7 ± 5.6 %). KO animals showed a slow continuous recovery to 80.6 ± 8.8 % at 28 days post injury, without showing a clear plateau within the timespan of this experiment.

Cylinder test

We analysed forelimb function using the cylinder test. Intact animals voluntarily explore the vertical wall using both forepaws in more than 90% of all rearing events. After lesioning the left RST, animals exhibited a strong preference in using their right paw only. On day 3 after injury, we observed an increased right paw usage of 38.4 ± 7.2 % and 55.2 ±12.9 % in WT and KO animals respectively (Fig. 4). WT animals recovered to 22.5 ±7.2 % on day 10, while in KO animals the deficit essentially remained the same until 14 days after injury. From day 21 after injury all animals performed equally without further improvement in paw usage (KO: 32.4 ± 8.1, WT: 32.4 ± 8.9). Similar to the rotarod test, as a result of a

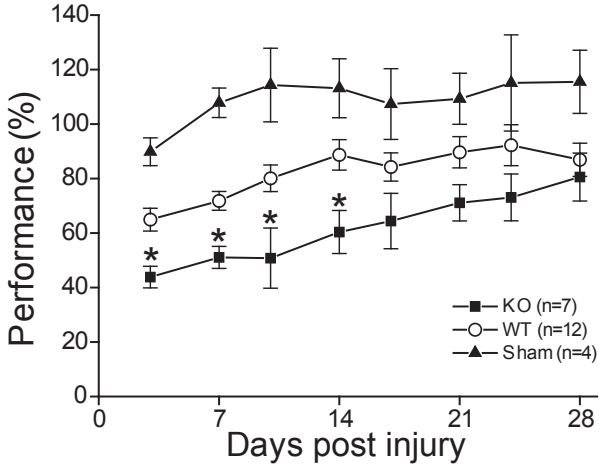

Figure 3. Decreased rotarod performance in Npn-2 KO mice after RST lesion. Three days after lesion of the left RST, rotarod the performance of KO animals showed a significantly larger deficit (43.8 ± 3.9%) than WT animals (64.9 ± 4.2%). WT animals gradually recovered, reaching a plateau performance level of 88.7 ± 5.6 % at 14 days post injury. The motor function of KO animals was significantly decreased as compared to WT animals until 14 days post injury and continued to slowly recover to 80.6 ± 8.8 % at 28 days post injury. (p<0.05 significance between KO and WT)*

lesion of the RST we unexpectedly found that KO animals showed an increased dysfunction as compared to WT animals.

Catwalk

Using the catwalk system, we quantitatively analysed several specific gait parameters: The stride length of both front and hind limbs was unaffected by the RST lesion. Intact and injured KO animals showed a significantly smaller front and hind limb stride length (Fig. 5a,b). The stand time, the duration a certain paw has contact with glass plate, was unaffected after injury to the RST. Although this parameter was not indicative for deficits in motor function that were caused by the lesion, it did show to be significantly increased in uninjured KO animals as compared to WT littermates (Fig. 6). The swing time, the duration between paw placements, was measured for the individual paws (Fig. 7a, b, c, d). Three days after injury, the swing time of the left forelimb was significantly increased in WT and KO animals as compared to sham-operated animals. This increase did not recover throughout the duration of the experiment (Fig. 7a). The swing time of the left hind limb was significantly increased in KO animals as compared to WT littermates 7 days after injury (WT: 119 ± 9 ms, KO: 184 ± 24 ms) (Fig. 7c). KO animals continued to show a trend of increased swing time as compared to WT animals until day 24, and recovered to the level of injured WT animals 28 days after injury.

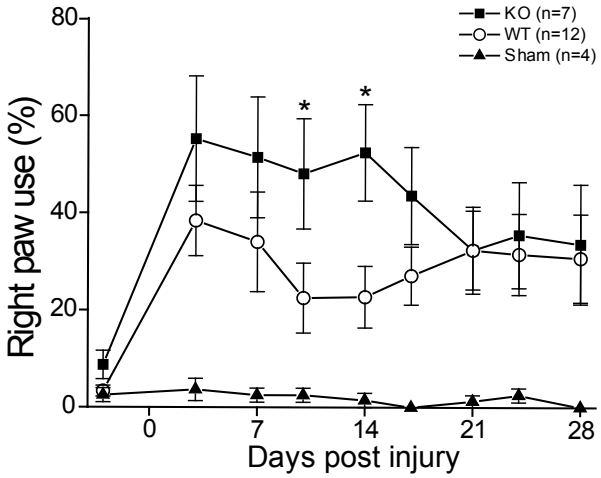

Figure 4. Increased right paw preference RST lesion In Npn-2 KO animals. After lesion of the left RST, Npn-2 KO animals showed an increased preference in right paw usage during spontaneous vertical rearing behaviour as compared to their WT littermates (KO: 55.2 ±12.9 %; WT, 38.4 ± 7.2 %). This increased preference was maintained until day 14 post injury and recovered to the WT level at day 21 after injury. (KO: 32.4 ± 8.1, WT: 32.4 ± 8.9). (p<0.05 significance between KO and WT)*

Discussion

In this study we have examined the regenerative response of Npn-2 KO mice after injury of the RST. Deletion of the Npn-2 gene has no effect on the regeneration of injured RST fibers. After RST injury, Npn-2 KO animals do not show an enhanced recovery of motor function. Similar to the Npn-1 conditional KO animals studied in chapter 5, Npn-2 KO mice show an increased loss of motor function as compared to control animals. Non-lesioned, intact Npn-2 KO animals have a smaller stride length and an increased stand time on the Catwalk gait analysis. The decreased stride length is likely due to their smaller size. Additional phenotypic differences in motor function between WT and Npn-2 KO mice are revealed after RST injury as shown by the decreased performance in the other functional tests used here. The precise mechanism underlying these phenotypic effects is unknown, but could be attributed to the observation that KO animals have developmental defects in cranial and spinal nerves. (Chen *et al.,* 2000, Giger *et al.,* 2000). In addition to its role in axonal guidance in the developing CNS, Npn-2 plays a role in spine density and synaptic activity in the adult CNS (Sahay *et al.,* 2005, Tran *et al.,* 2009). Therefore normal neuronal function may be affected in Npn-2 KO animals.

With the exception of Sema3E, the other four class 3 semaphorins that are expressed in the neural scar signal by binding to Npn-1 or Npn-2. In WT animals, neurons of the red nucleus express only Npn-2. As a result, the RST fibers in Npn-

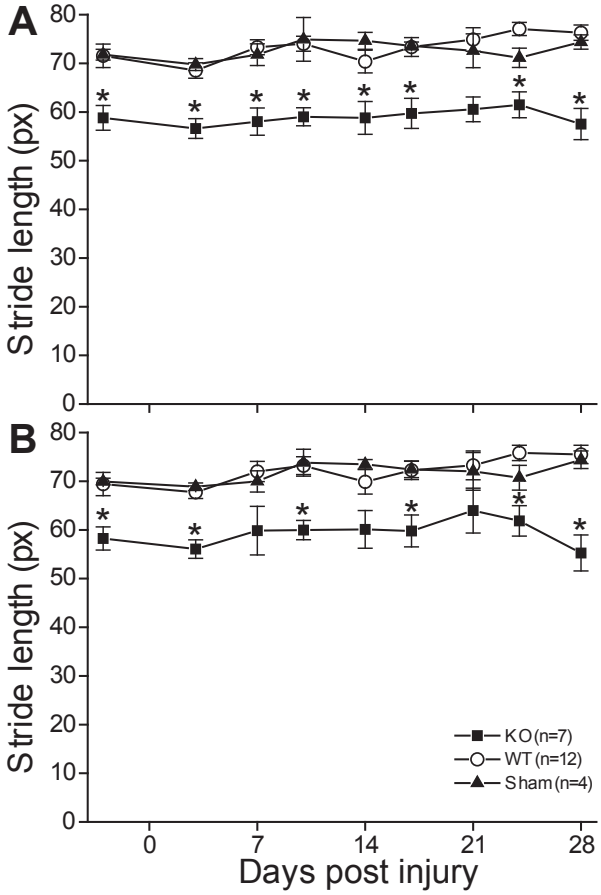

*Figure 5. The stride length is unaffected by RST lesion. Intact, uninjured Npn-2 KO animals show a decreased stride length in front (a) and hind limbs (b) as compared to WT littermates. The stride length did not change after RST lesion. (*p<0.05 significance between KO and WT)*

2 KO animals are considered to be unresponsive to most class 3 semaphorins. By studying RST fiber regeneration in the Npn-2 KO mouse it is possible to determine the combined contribution of the majority of class 3 semaphorins to the inability of the RST to regenerate. Unexpectedly, both RST fiber regeneration and motor function was not enhanced in RST lesioned Npn-2 KO animals.

There are at least 3 possible reasons by which these negative results could be explained. First, the presence of receptors for other growth inhibitory proteins, including receptors for myelin inhibitors, ephrins, slits and RGMa may continue to suppress regenerative growth of injured RST fibers. A first attempt to simultaneously compromise signalling by two classes of inhibitors has recently been reported in a study by Lee et al. In PlxA4/PlxA3/Nogo receptor-1 triple knockout mice, raphe spinal and corticospinal fibers did not show improved axon regeneration after complete spinal cord transection (Lee *et al.,* 2010a). Thus,

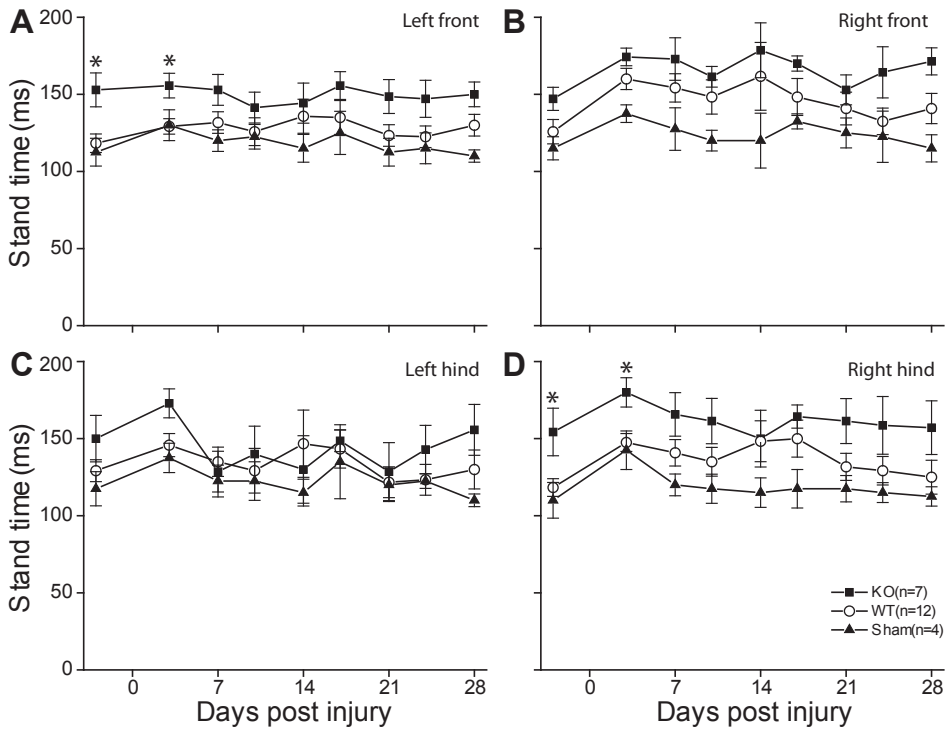

Figure 6. The stand time is unaffected by RST lesion. Injury to the left RST does not significantly affect the stand time of the individual paws (a, b, c, d) of KO and WT animals. Uninjured KO animals show an increased stand time as compared to WT animals. (p<0.05 significance between KO and WT)*

the simultaneous attenuation of the semaphorin and nogo signalling pathways by the constitutive genetic mutation of specific components of the multimeric receptor did not result in a measurable regenerative response. However, even in this triple transgenic animal the signalling pathways of three other repulsive protein families (ephrin, slit, RGM) are still intact.

Second, Npn-2 is a receptor for splice forms of VEGF (Gluzman-Poltorak *et al.,* 2000) and some forms of VEGF also have neurotrophic activity (Sondell *et al.,* 1999, Matsuzaki *et al.,* 2001, Yasuhara *et al.,* 2004). Constitutive KO of Npn-2 in neurons may render these cells insensitive to two factors with opposing effects, namely lack of a neurotrophic or neuroprotective influence (VEGF) and a chemorepulsive effect (semaphorins). In this scenario, neutralisation of semaphorins in the scar would by effective, since it would selectively remove the repulsive component and would leave the beneficial signal (VEGF) for the Npn-2 receptor intact. Third, constitutive knockout of Npn-2 in other cells than neurons (including blood vessel, lymph vessel and scar cells) may have effects on scar formation and/or wound healing. In Npn-2 knockout animals, new blood vessel formation in the retina was suppressed after an ischemic lesion (Shen *et al.,* 2004). Similar effects may have occurred after a spinal cord lesion and this

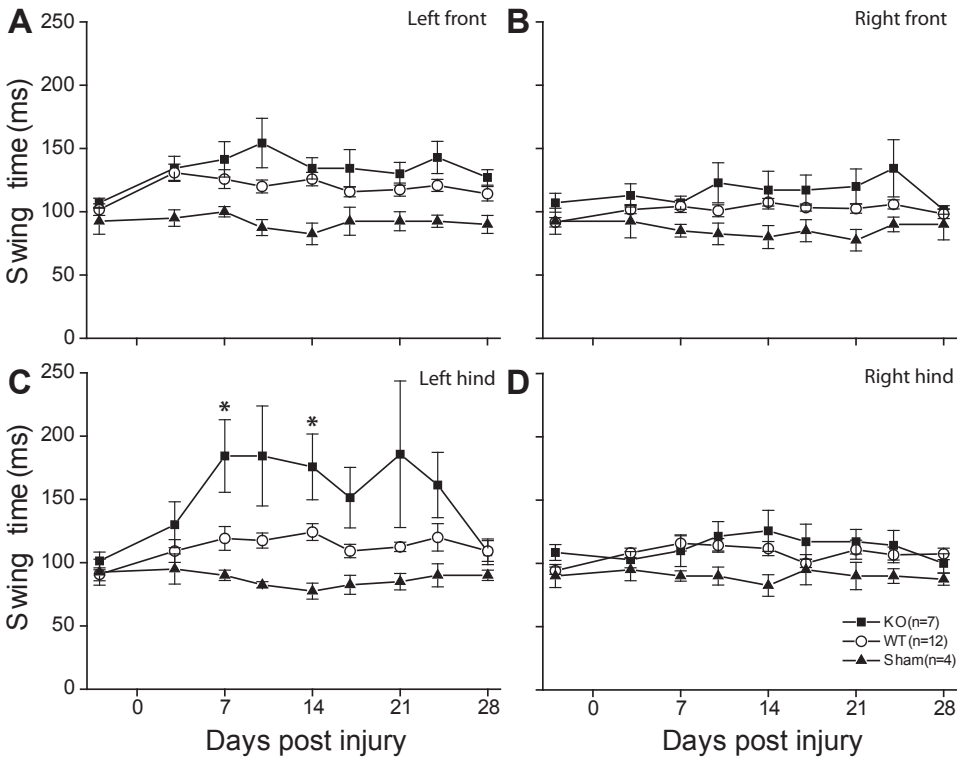

Figure 7 – Increased swing time in Npn-2 KO mice after RST injury. Three days after injury of the left RST, the swing time of the left forelimb of injured WT and KO animals is significantly increased as compared to sham operated animals, which did not recover throughout the duration of the experiment (fig 7a). The swing time of the left hind limb was significantly increased in KO animals as compared to WT littermates 7 days after injury (WT: 119 ± 9 ms, KO: 184 ± 24 ms) (fig 7c). KO animals continued to show an increased swing time as compared to WT animals until day 24. (p<0.05 significance between KO and WT)*

may "mask" the role of neuronal Npn-2 in the repulsion of injured RST axons per se.

In the PNS axonal regeneration through a sciatic nerve crush site was delayed in Npn-2 knockout mice (Bannerman *et al.,* 2008). This indicates that Npn-2 expression has a beneficial effect on axon regeneration following a lesion that does not result in scar formation and allow regeneration of axons along a pathway of growth promoting Schwann cells. Studies on the role of Npn-2 in injured CNS and PNS neurons and in the various cell types in a non-permissive spinal cord scar and a permissive denervated sciatic nerve will have to be executed to further our understanding of the role of Npn-2 in neuroregeneration.